

Supporting Information for:

New insights into the nitroaromatics-detection mechanism of the luminescent metal-organic framework sensor

*Lei Liu,^{ab} Xiaofang Chen,^b Jieshan Qiu^a and Ce Hao^{*a}*

^a State Key Laboratory of Fine Chemicals, Dalian University of Technology, Dalian 116024, China.

^b State Key Laboratory of Molecular Reaction Dynamics, Dalian Institute of Chemical Physics, Chinese Academy of Sciences, Dalian 116023, China.

Page Contents:

Page 2: Figure S1, structure of the organic linker L; Figure S2, pictures of the cluster models.

Page 3: Figure S3, detailed fragment orbital interaction diagram for CL-NB-MOF cluster.

Page 4: Figure S4, detailed fragment orbital interaction diagram for CL-Ben-MOF cluster.

Page 5: Figure S5, detailed fragment orbital interaction diagram for CL-AC-MOF cluster.

Page 6: Table S1, calculated lattice parameters and corresponding experimental data; optimization of the crystal structures.

Page 7: Table S2, binding energies for the adsorbates.

Page 8: Table S3, Table S4 excitation energies for the clusters.

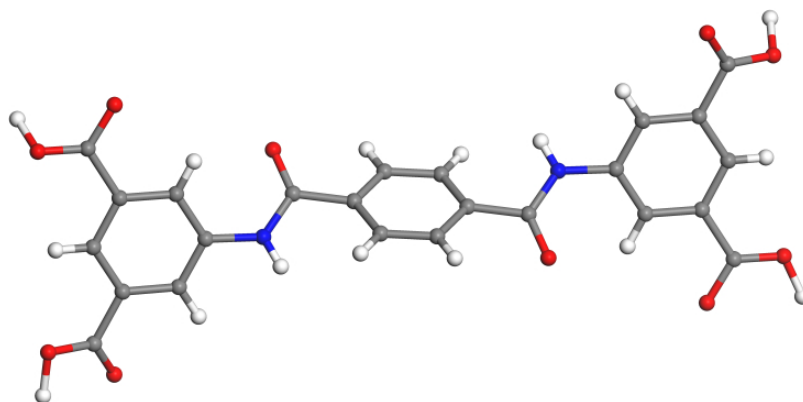


Figure S1. Structure of the H₄L (bis-(3,5-dicarboxy-phenyl)terephthalamide) ligand.

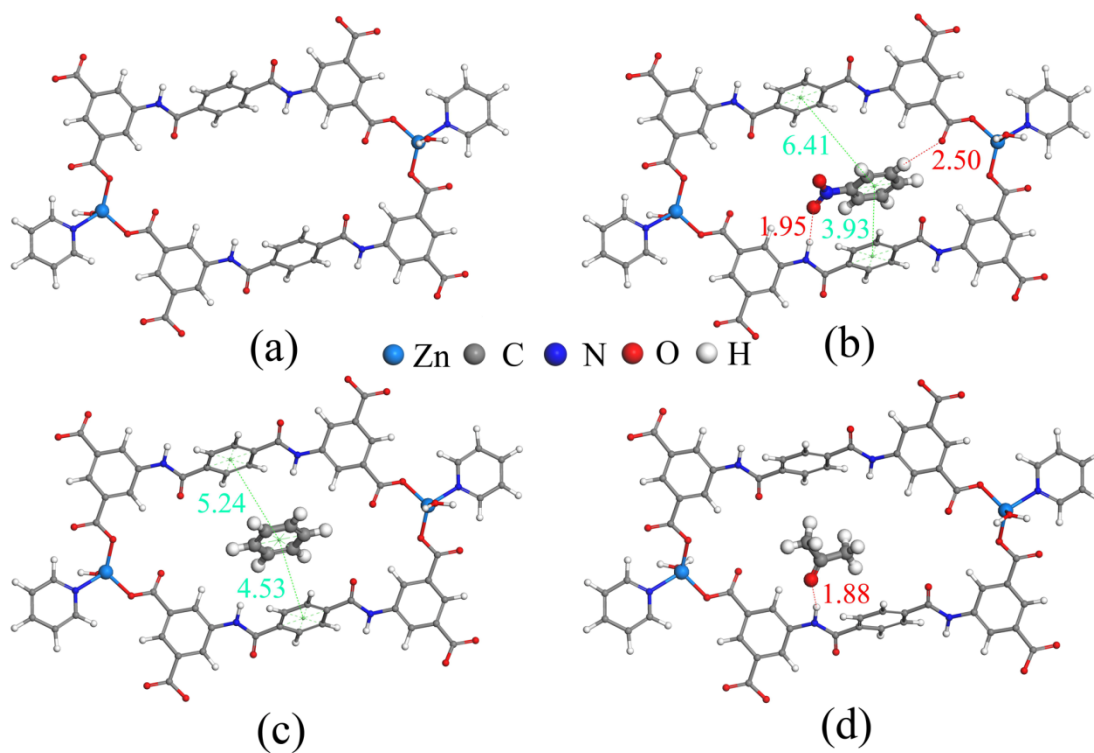


Figure S2. Cluster models for (a) LMOF **1**, (b) NB-MOF, (c) Ben-MOF and (d) AC-MOF. Hydrogen bond lengths are given in red fonts and centroid distances between aromatic rings are given in cyan fonts.

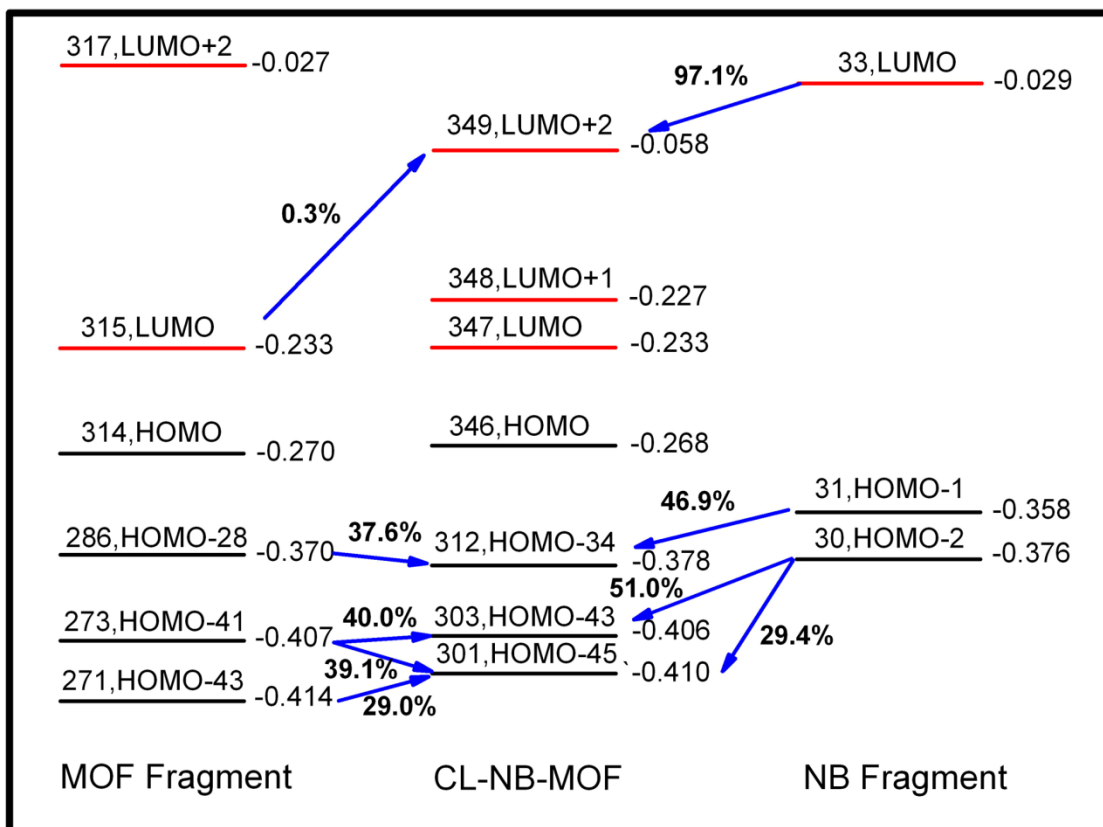


Figure S3. Detailed fragment orbital interaction diagram for CL-NB-MOF. Contributions of the fragment orbitals to corresponding complex orbitals are given around the blue arrows. Energy values (Hartree) for each orbit are listed beside the corresponding orbitals.

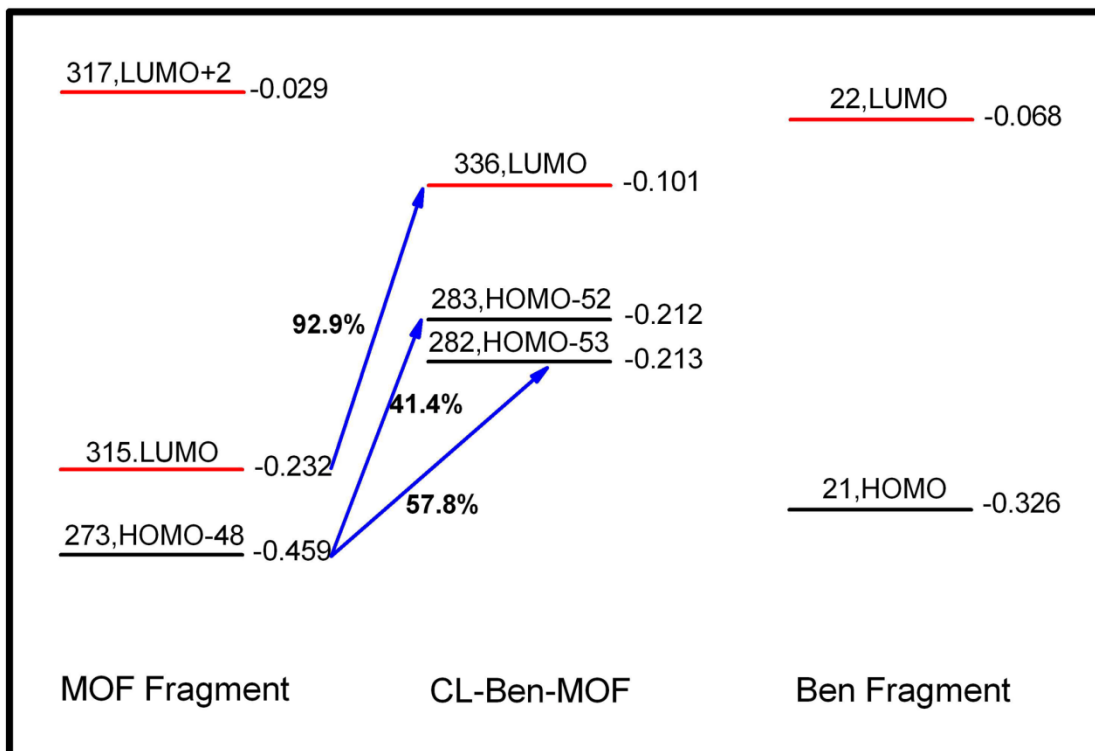


Figure S4. Detailed fragment orbital interaction diagram for CL-Ben-MOF. Contributions of the fragment orbitals to corresponding complex orbitals are given around the blue arrows. Energy values (Hartree) for each orbit are listed beside the corresponding orbitals.

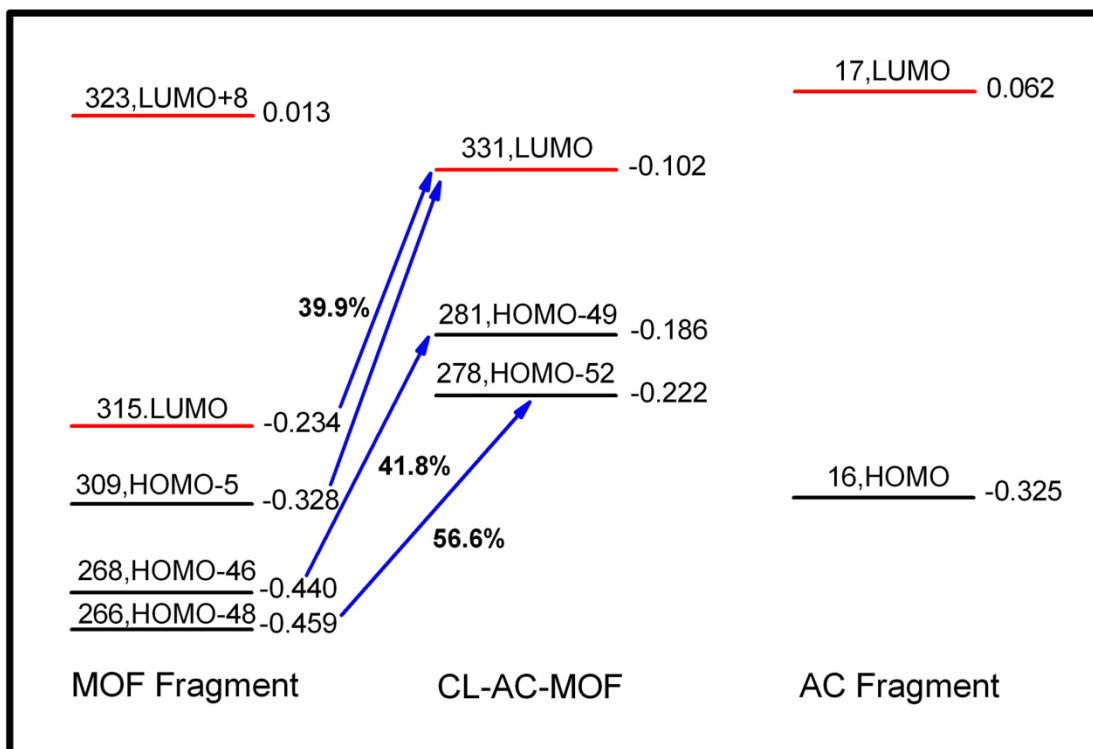


Figure S5. Detailed fragment orbital interaction diagram for CL-AC-MOF. Contributions of the fragment orbitals to corresponding complex orbitals are given around the blue arrows. Energy values (Hartree) for each orbit are listed beside the corresponding orbitals.

Table S1. Calculated lattice parameters and corresponding experimental data. Deviations from experimental data are shown in parentheses.

Lattice Parameter	CASTEP/PBE	CASTEP/PW91	Dmol3/PBE/DNP	expt ^a
a (Å)	9.7 (2%)	9.7 (2%)	9.6 (1%)	9.5
b (Å)	9.7 (1%)	9.7 (1%)	9.7 (1%)	9.6
c (Å)	13.5 (5%)	13.5 (5%)	13.4 (5%)	12.8
α (degrees)	92.5 (3%)	92.8 (3%)	93.3 (3%)	95.8
β (degrees)	93.5 (2%)	93.5 (2%)	92.6 (1%)	91.9
γ (degrees)	114.0 (2%)	114.2 (2%)	113.2 (1%)	111.7

^aExperimental data obtained from ref 22.

Optimizations of the Crystal Structures: The crystal structure for LMOF 1 was optimized using the experimentally determined single-crystal X-ray diffraction structure as the starting geometry²². Three different theoretical methods were used to generate the unit cell structures and compared with experimental data to test the credibility of our calculation results (namely CASTEP/PBE, CASTEP/PW91, DMol3/PBE/DNP). As reported in Table S1, the calculated lattice parameters a , b , β , γ are within an error of 2% compared to the experimental data. For c and α , the errors are a little bigger (5% and 3% respectively). These errors may originate from the fact that the calculations were performed at 0K in vacuum with water solvent while the experiment results were obtained at room temperature in the air. Anyway, all the errors are among the acceptable region considering the complexity of the MOF structure which would have neglectable effect on the results of our research. Besides, the fact that three different theoretical approaches predict nearly identical crystal structures gives us further confidence in the reliability of the theory.

Table S2. Calculated absolute energies and the corresponding binding energies^a for the three adsorbates.

Structure	Analyte	Framework	Total Energy	Binding energy
NB-MOF	-2151.219252452	-32686.61725572	-34838.90484197	1.068
Ben-MOF	-1024.995367498	-32686.37407084	-33712.06084054	0.691
AC-MOF	-998.1446741799	-32686.65911294	-33685.65572994	0.852

^aThe binding energies are obtained by using the following equation: $E_{\text{interaction}} = E_{\text{LMOF}} + E_{\text{analyte}} - E_{\text{LMOF+analyte}}$. All the energies are given in electron volt (eV).

Table S3. Selected calculated electronic transition energies, corresponding oscillator strengths (f), orbital contributions (contrib), compositions (comp) and transition characters (character) of the singlet excited states of the four clusters.^a

Cluster	Transition	abs. (nm/eV)	f	contrib	comp	character
CL-LMOF 1	$S_0 \rightarrow S_{86}$	342.8/3.62	0.0001	H-41 \rightarrow L	35.4%	LLCT, ILCT
				H-40 \rightarrow L+1	32.4%	LLCT, ILCT
	$S_0 \rightarrow S_{87}$	340.2/3.64	0.0044	H-49 \rightarrow L+1	31.6%	LLCT, ILCT
				H-48 \rightarrow L	31.9%	LLCT, ILCT
	$S_0 \rightarrow S_{88}$	340.2/3.64	0.0000	H-49 \rightarrow L+1	31.8%	LLCT, ILCT
				H-48 \rightarrow L	32.1%	LLCT, ILCT
CL-NB-MOF	$S_0 \rightarrow S_{93}$	344.2/3.60	0.0016	H-58 \rightarrow L	25.4%	LLCT
				H-47 \rightarrow L+1	23.2%	LLCT
	$S_0 \rightarrow S_{94}$	343.4/3.61	0.0025	H-45 \rightarrow L+2	34.9%	MOF \rightarrow analyte, HB
				H-43 \rightarrow L+2	49.7%	MOF \rightarrow analyte, HB
				H-34 \rightarrow L+2	4.3%	MOF \rightarrow analyte, π - π
	$S_0 \rightarrow S_{95}$	342.8/3.61	0.0013	H-57 \rightarrow L+1	19.1%	LLCT, ILCT
CL-Ben-MOF	$S_0 \rightarrow S_{90}$	341.1/3.63	0.0000	H-43 \rightarrow L	90.9%	LLCT
	$S_0 \rightarrow S_{91}$	339.0/3.66	0.0026	H-53 \rightarrow L	23.5%	LLCT, ILCT
				H-52 \rightarrow L	32.4%	LLCT, ILCT
	$S_0 \rightarrow S_{92}$	338.9/3.66	0.0018	H-53 \rightarrow L+1	29.2%	LLCT, ILCT
H-52 \rightarrow L+1				26.2%	LLCT, ILCT	
CL-AC-MOF	$S_0 \rightarrow S_{85}$	353.8/3.50	0.0000	H-37 \rightarrow L	67.1%	LLCT
	$S_0 \rightarrow S_{86}$	346.2/3.58	0.0014	H-41 \rightarrow L	81.0%	LLCT
	$S_0 \rightarrow S_{87}$	345.6/3.59	0.0021	H-52 \rightarrow L	33.7%	LLCT, ILCT
				H-49 \rightarrow L	25.0%	LLCT, ILCT
$S_0 \rightarrow S_{92}$	344.7/3.60	0.0003	H-45 \rightarrow L+1	92.3%	LLCT	

^aLLCT represents ligand to ligand charge transfer, ILCT represents intra-ligand charge transfer, “MOF \rightarrow Analyte, HB” represents electron transfer from MOF to analyte molecule via hydrogen bond and “MOF \rightarrow Analyte, π - π ” represents electron transfer from MOF to analyte via π - π stacking.

Solvent effects are not included in this article based on the fact that the experiment²² was carried out in an acetonitrile suspension and LMOF 1 is not soluble. However, the solvated excitation energies are obtained with the self-consistent reaction field (SCRf) method in a polarizable continuum model (PCM) with acetonitrile as solvent for comparison. As shown in Table S4, the excitation energy for the non-solvated model of CL-MOF 1 shows better agreement with the experimental value which further confirmed the validity of this method.

Table S4. Values for the non-solvated and solvated excitation energies for CL-MOF 1.

	Transition	abs. (nm)	f
Non-Solvated Model	$S_0 \rightarrow S_{87}$	340.2	0.0044
Solvated Model	$S_0 \rightarrow S_{86}$	327.4	0.0036
Experimental Value ^a	—	350	—

^aExperimental values obtained from reference 22.